$^{209}Bi + ^{136}Xe$ reaction at $E_{lab} = 1422$ MeV

H.J. Wollersheim,* W. W. Wilcke, J. R. Birkelund, J. R. Huizenga, and W. U. Schröder
Nuclear Structure Research Laboratory and Departments of Chemistry and Physics, University of Rochester, Rochester, New York 14627

H. Freiesleben†
Gesellschaft für Schwerionenforschung, D-6100 Darmstadt, Germany

D. Hilscher
Hahn-Meitner-Institut für Kernforschung, D-1000 Berlin, Germany
(Received 6 July 1981)

Projectilelike reaction products from the $^{209}Bi + ^{136}Xe$ reaction were studied at a laboratory bombarding energy of 1422 MeV. The fragments were identified by atomic number, and their kinetic energies and angular distributions were measured using three solid-state ΔE-E telescopes. The strongly damped products exhibit features similar to those seen in two previous measurements of the same reaction at 940 and 1130 MeV. The angular distribution is peaked near the grazing angle. The minimum kinetic energy is bombarding-energy independent and 150 MeV smaller than the Coulomb energy of touching spherical fragments, indicating a large deformation of these dinuclear systems. The measured element distributions for given Q values are found to be Gaussian and centered at the atomic number of the projectile. At large negative Q values, the centroids of the Gaussian distributions exhibit a small drift towards charge splits more asymmetric than the initial system. Various correlations between experimental observables, including the variances of the Z distributions, the centroids of the angular distributions, and the Q values, are interpreted for all three bombarding energies in terms of the proximity one-body transport model. The experimental relations are satisfactorily reproduced by this theory.

[NUCLEAR REACTIONS $^{209}(^{136}Xe,HI)$; $E_{lab} = 1422$ MeV; one-particle inclusive measurement of $\sigma(E,Z,\theta)$; strongly damped reaction; extracted first and second moments of element distributions and centroids of angular distributions as a function of Q value; comparison with proximity one-body transport model.]

I. INTRODUCTION

The study of damped collisions between heavy ions at energies a few MeV per nucleon above the Coulomb barrier has revealed a variety of new reaction phenomena[1] intermediate between those pertaining to direct and compound nucleus processes. Two experimental methods are currently used to gain further insights into the damped reaction mechanism: (i) studies of different systems keeping the ratio of the center-of-mass energy to the Coulomb barrier fixed; and (ii) investigations of the bombarding-energy dependence of the reactions induced by one target-projectile combination.

It is the purpose of this work to extend the previous studies[1,2] of the $^{209}Bi + ^{136}Xe$ reaction to a higher bombarding energy of 1422 MeV. Since relatively few reactions have been measured in detail over a wide range of bombarding energies, this well-investigated system has been chosen for studying the bombarding-energy dependence of the reaction properties. In the previous experiments at 940 and 1130 MeV the observed sideways-peaked angular distribution can be attributed to a delicate balance between the attractive nuclear forces and the repulsive Coulomb forces. Raising the bombarding energy is expected to alter this balance of forces and should change the deflection function from a

focusing to an orbiting type. At the same time the amount of total kinetic energy (i.e., $E=E_{c.m.}+Q$ value), which can be dissipated in the reaction, is also increased by more than a factor of 2 as compared to the 940 MeV experiment. With increasing bombarding energy, one expects a deeper interpenetration of the two nuclei for the same impact parameter such that model predictions can be tested in a more interior region of the nuclear potential. The most interesting feature to be studied is the correlation between the dissipated energy and the fragment Z distributions. At the lowest bombarding energy a classical one-body dissipation model[1] fails to reproduce this experimental relation, which has been attributed[2,3] to the neglect of the fermion nature of the exchanged nucleons. This quantal effect is predicted to be strongly bombarding-energy dependent. Hence, the present work, in combination with the experiments performed at lower bombarding energies, provides a sensitive test of these model assumptions.

In the following section, measurements and data evaluation are briefly described. Results on elastic scattering and the gross features of the one-fragment inclusive measurements such as angular, atomic number, and energy distributions for the Xe-like reaction products are discussed in Sec. III. In Sec. IV, various experimental quantities, transformed into the center-of-mass system, are compared with theoretical predictions of a one-body transport model. Included in these comparisons are the moments of the scattering angle and atomic number distributions of the light (Xe-like) fragment as a function of the negative Q value ($\equiv$ total kinetic energy loss E_{loss}). Conclusions are presented in Sec. V.

II. EXPERIMENTAL PROCEDURE

The experiment was performed at the UNILAC of the GSI laboratory in Darmstadt. Self-supporting targets of 490 μg/cm^2 ^{209}Bi were bombarded with 1422 MeV ^{136}Xe ions. Three ΔE-E telescopes, each consisting of two solid-state detectors, were used to identify the atomic number of the projectilelike fragments measured in the angular range between 11° and 30° in the laboratory frame, in steps of about 1°. The telescopes subtended angles of 0.5° in the reaction plane. The thicknesses of the transmission detectors used were 14.8, 19.0, and 19.3 μm, respectively, whereas the thickness of the stop detectors was 150 μm for the two forward telescopes and 100 μm for the third telescope. The relative normalization of data taken at different angles was achieved by using the count rate of two surface barrier detectors mounted at a scattering angle of $\pm 14°$ above the reaction plane. The energy calibration of the system was obtained by means of an alpha source and a precision pulse generator. The energy resolution of each telescope was typically 4.5% FWHM for elastically scatttered Xe ions.

Standard electronics were used in the experiment, as described elsewhere.[1] It included pileup circuitry and a system that allowed a determination of dead-time corrections. The ΔE-E energy signals from the telescopes were recorded by the GSI PDP-11/45 online computer system and stored event by event on magnetic tape. The analysis of the data was performed with the PDP-10 computer of the University of Rochester.

The particle identification was carried out, event by event, on the basis of an energy loss (dE/dx) theory given by Braune and Schwalm.[4] In this theory, the energy loss of heavy ions in solids (e.g., silicon) is given by a semiempirical formula, thus avoiding the necessity of an extended tabulation of theoretical $dE/dx(Z,E)$ values or experimental $\Delta E/\Delta x(Z,E)$ values, which would have to be measured for every transmission detector separately. The analytical formula, however, underestimates the experimental energy loss values and the particle energy corresponding to the maximum of the energy loss curve, as observed in Ref. 5. For the present application, these discrepancies can be corrected, if one parametrizes the specific energy loss as suggested by Schwalm[6] according to

$$-\frac{dE}{d(\rho x)}=k_n(V_0/V)+k_e(V/V_0)+k_3(V/V_0)^3, \quad (V\le V_{cut}), \quad \text{(1a)}$$

$$-\frac{dE}{d(\rho x)}=a+b(V/V_0)+c(V/V_0)^2, \quad (V\ge V_{cut}). \quad \text{(1b)}$$

The quantity ρ is the density of the stopping material ($\rho_{Si}=2.33$ g/cm^3), V is the velocity of the moving ion, and V_0 is the velocity of light divided by 137. While k_n was taken from Warburton *et al.*,[7] k_e and k_3 were chosen to match the two equations smoothly at $V=V_{cut}$. The Z-dependent parameters a, b, and c were obtained by a least-squares fit to the theoretical energy loss calculated as described in Ref. 4. The remaining parameter V_{cut} has a strong influence on the shape of the energy loss curve. This fact is used to fit the theoret-

ical function [Eq. (1)] to eight measured energy loss curves of $\Delta E/\Delta x$ versus E_{total} for ions with $Z=18$, 26, 36, 54, and 82 and Δx between 7.9 and 14.8 μm in order to determine V_{cut}. The result seems to be independent of detector thickness and can be parametrized by

$$V_{\text{cut}}=5.032+0.144Z-4.419\times10^{-4}Z^2 . \quad (2)$$

The remaining deviations between experimental and theoretical $\Delta E/\Delta x$ values can be eliminated by introducing an effective thickness for the transmission detector, which is slightly larger than the value measured by the energy loss of α particles.

This energy loss formula was applied in order to convert the experimental ΔE-E distributions into Z-E_{total} distributions. The energy deposited in the E counter of each telescope was corrected for the pulse height defect using a power-law formula given by Moulton *et al.*[8] The different values of the intrinsic Z resolutions of the three telescopes ranging from 2.2 to 4.4 units FWHM were matched to the latter value by folding the energy-dependent element distribution with a Gaussian, a procedure which allowed a combination of all data.

The three measured quantities of the projectile-like fragment, atomic number Z, final kinetic energy, and scattering angle, were transformed into the center-of-mass system assuming two-body kinematics and a fragment mass-to-charge ratio equal to that of the combined system, which for this reaction is equal to those of both ^{209}Bi and ^{136}Xe individually. The effect of neutron evaporation on the reconstructed Q value was taken into account by assuming that one neutron is emitted per 12 MeV of excitation energy. A Q value bin width of 50 MeV, used in the following sections, seems to be reasonable in view of the experimental energy resolution.

III. EXPERIMENTAL RESULTS AND DISCUSSION

A. Elastic scattering angular distribution

One of the objects of investigating the elastic scattering of ^{136}Xe from a ^{209}Bi target in the present experiment was to determine the total reaction cross section, in order to estimate the yield missing due to the limited angular range of observation. Using the technique of separating the elastic intensity from the quasielastic component described in Ref. 9, the ratio of the elastic to the Rutherford cross section as a function of the c.m. scattering angle was calculated and the results are shown in Fig. 1. The errors of the measured differential cross sections include not only the statistical uncertainties, but also estimated systematical errors due to incomplete separation of the elastic peak. Since the energy resolution in these measurements precludes a determination of a pure elastic scattering cross section, it should be emphasized that the events labeled as elastic encompass Q values in the range from -20 to $+20$ MeV. It should be noted, however, that only for this definition of "elastic" scattering can the onset of the nuclear forces be described as a function solely of bombarding energy, masses, and atomic numbers of the projectile-target combination. The study of individual states, e.g., the ground state, requires additional information about the detailed properties of nuclear structure.

The quarter-point angle for $E_{\text{lab}}=1422$ MeV is found to be $\theta_{1/4}(\text{lab})=23.2°\pm0.5°$ [$\theta_{1/4}(\text{c.m.})=38.0°\pm0.9°$], where the quoted error is due to the statistical uncertainty in determining the slope of $d\sigma_{\text{el}}/d\sigma_{\text{Ruth}}$ from the measured cross sections. Applying the generalized Fresnel diffraction model[10] to these data, the angular momentum l_g

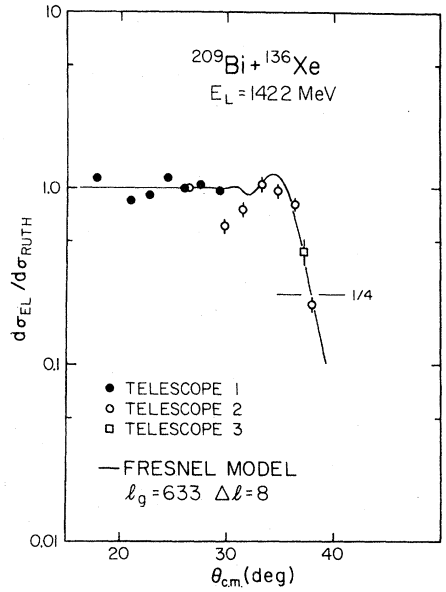

FIG. 1. Ratio of the experimental elastic scattering cross section (including inelastic events with Q values larger than -20 MeV) to the Rutherford cross section as a function of the center-of-mass angle $\theta_{\text{c.m.}}$. The solid line is generalized Fresnel model fit (Ref. 10) to the data with the listed parameters.

TABLE I. Characteristic parameters of the ^{209}Bi+^{136}Xe reaction at 940, 1130, and 1422 MeV. A number of the listed quantities are derived from the experimental $\theta_{1/4}$(c.m.) angle using the generalized Fresnel model (Ref. 10).

Quantity	940 MeV	1130 MeV	1422 MeV	Units
E_{lab}	940	1130	1422	MeV
$E_{c.m.}$	569	684	861	MeV
$\theta_{1/4}$(lab)	43.5°	33°	23.2°	deg
$\theta_{1/4}$(c.m.)	70.1°	54°	38.0°	deg
μ (reduced mass)	82.4	82.4	82.4	u
k_∞ (wave number)	47.37	51.94	58.26	fm^{-1}
η (Coulomb parameter)	268.4	244.8	218.2	
η' (Ref. 13)	519	400	306	
R_{int} (Fresnel)	15.5	15.1	15.2	fm
l_g (Fresnel)	383	480	633	$\hbar$
σ_R (Fresnel)	2.06	2.70	3.8	b
σ_R(exp)	2.09	2.80	3.1	b
$V_C(R_{int})$	416	428	423	MeV
$T_0=E_{c.m.}-V_C(R_{int})$	152	256	438	MeV
$[E_{c.m.}-V_C(R_{int})]/\mu$	1.86	3.11	5.32	MeV/nucleon
peak in $d\sigma_R/d\Omega$(lab)	39.5°	30°	20°	deg
peak in $d\sigma_R/d\Omega$(c.m.)	64.5°	50°	34°	deg

for a grazing collision, the interaction radius R_{int}, the corresponding Coulomb barrier $V_c(R_{int})$, and a total reaction cross section of $\sigma_R=(3.8\pm0.2)$ b are derived. If systematic uncertainties are taken into account, the error bar of the total reaction cross section increases to ±0.4 b. Values for these and other parameters are listed and compared in Table I for the ^{209}Bi+^{136}Xe reaction at laboratory bombarding energies of 940, 1130, and 1422 MeV.

B. Angular distributions of Xe-like reaction fragments

The differential reaction cross section $d\sigma/d\Omega_{lab}$ for the Xe-like reaction fragments from the ^{209}Bi+^{136}Xe reaction at 1422 MeV is plotted in Fig. 2 versus laboratory angle. The integration of the angular distribution yields a cross section of $\sigma_R=(3.1\pm0.4)$ b, deviating only by about 18% from the value deduced from the Fresnel model analysis of elastic scattering data. Part of this difference might be due to the fact that no data were taken for laboratory angles smaller than 11°. The above approximate agreement in the measured and Fresnel total reaction cross section suggests that nearly all of the Xe-like reaction fragments are focused into the narrow angular region ($11°\leq\theta_{lab}\leq30°$) covered by the three telescopes.

Similar to the results from the 940 and 1130 MeV experiments, the differential reaction cross section is observed to be peaked at an angle slightly forward of the quarter-point angle. However, the angular distribution measured at a bombarding ener-

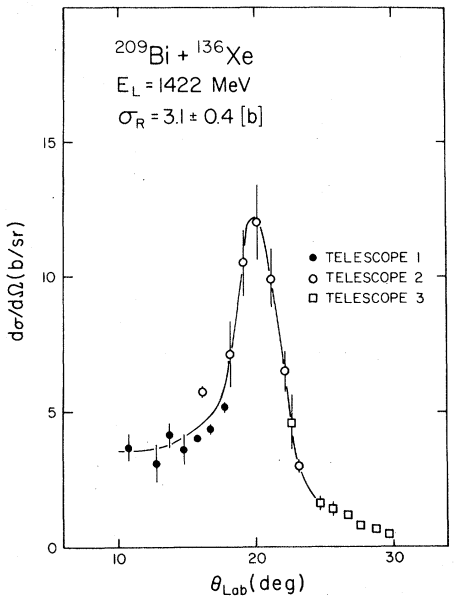

FIG. 2. Laboratory angular distribution for the Xe-like fragments. A curve has been drawn through the data points to guide the eye.

gy of 1422 MeV shows a slight forward asymmetry, a result which is not unexpected, in view of the trend established by the measurements at $E_L = 940$ and 1130 MeV.

In Fig. 3 the angular distribution in the center-of-mass system is shown for all reaction events with a total kinetic energy E between 260 and 810 MeV. These events are all Xe-like reaction fragments; contributions from recoiling targetlike fragments are not detected because their grazing angle in the laboratory system is far out of the observation range. In addition, fragments resulting from sequential fission of Bi-like reaction partners are distinguished from damped reaction products because of their low kinetic energies in the laboratory.

C. Charge distribution of the Xe-like reaction fragments

The element distribution of the Xe-like fragments, integrated over the range of total kinetic energies mentioned above and over all observed scattering angles ($18° \leq \theta_{c.m.} \leq 128°$), is exhibited in Fig. 4. A comparison of the present data with that of two earlier investigations of this reaction shows that the maximum of the Z distribution remains centered at approximately the Z of the projectile for all bombarding energies, while its width increases with bombarding energy. The shape of the Z distribution is found to be nearly symmetric. A pronounced skewness in this distribution, as observed for the $^{166}Er + ^{86}Kr$ reaction at 12.1 MeV/nucleon[11] and interpreted as due to projectile fission, is not observed for the present $^{209}Bi + ^{136}Xe$ reaction at 10.5 MeV/nucleon.

D. Kinetic energy distribution

The large amount of kinetic energy dissipated in the $^{209}Bi + ^{136}Xe$ reaction at the three bombarding energies is illustrated in Fig. 5. The arrows represent the kinetic energies above the Coulomb barrier that are initially available, as calculated for spherical nuclei at the interaction radius, i.e., $E_{c.m.} - V_C(R_{int})$. The considerable fraction of the cross section below this Q value ($\equiv -E_{loss}$) clearly demonstrates that entrance and exit channels of the strongly damped collision process can be very different with respect to nuclear deformation, indicating the occurrence of very elongated configurations prior to scission. The degree of fragment deformation at separation can be estimated from the Q value. However, it should be remembered that, above all, the somewhat uncertain multiplicity for light-particle emission introduces a non-negligible error for large Q values. Independent of the bombarding energy a minimum kinetic energy $E = E_{c.m.} + Q$ of (270±30) MeV is observed for the

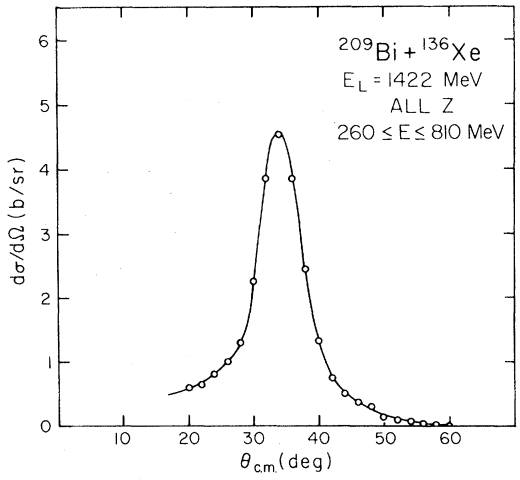

FIG. 3. Angular distribution in the center-of-mass system for light reaction products integrated over Q values in the range $-600 \leq Q \leq -50$ MeV. The distribution accounts for a reaction cross section of 2.8 b.

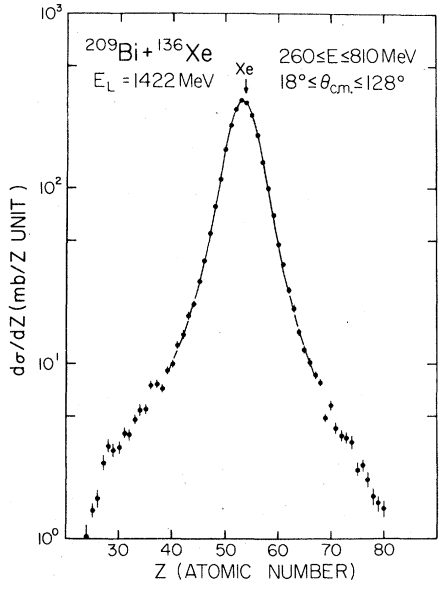

FIG. 4. Element distribution $d\sigma/dZ$ (integrated over $\theta_{c.m.}$ and total kinetic energy) plotted vs Z. The arrow indicates the charge of the projectile.

reaction fragments. This energy corresponds to a Coulomb energy of charge centers separated by (24±3) fm. The magnitude of the elongation of the stretched configuration appears to be similar to that in the normal fission process and can be appreciated by comparing the above distance to the interaction radius of $R_{int}=15$ fm, where nuclear reactions first start to occur in the entrance channel.

For symmetric fission the available kinetic energy of the fragments can be calculated using an empirical formula given by Viola.[12] An additional factor $4Z_PZ_T/(Z_P+Z_T)^2$ takes account of the fact that the average charges of the damped reaction products are close to those of the target and projectile, corresponding more to the case of asymmetric fission. For the reaction ^{209}Bi+^{136}Xe the above systematics predicts a minimum kinetic energy of 295 MeV, which is in good agreement with the measured value.

This result, as well as the observed fragment Z distribution, is reminiscent of features encountered in nuclear fission, while the angular distribution, on the other hand, is similar to that of a direct or relatively fast reaction, which clearly exemplifies the intermediate characteristics of damped reactions.

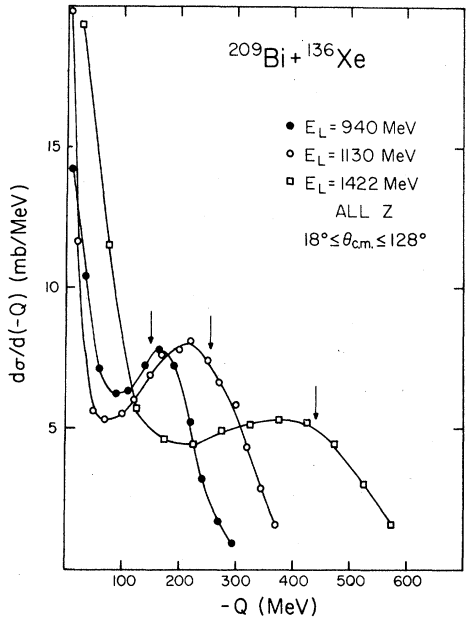

FIG. 5. Differential cross section $d\sigma/d(-Q)$ in mb/MeV as a function of the dissipated energy $(-Q)$. The damped events are integrated over all light fragments and reaction angles for the ^{209}Bi+^{136}Xe reaction at E_{lab}=940, 1130, and 1422 MeV. The arrows indicate the available kinetic energy in the entrance channel, i.e., $E_{c.m.}-V_C(R_{int})$.

E. Wilczyński and diffusion diagram

A convenient way to visualize the overall experimental results is provided by contour maps of the differential cross section as a function of two different sets of observables. Figures 6(a) and (b) show contour plots of the double-differential cross

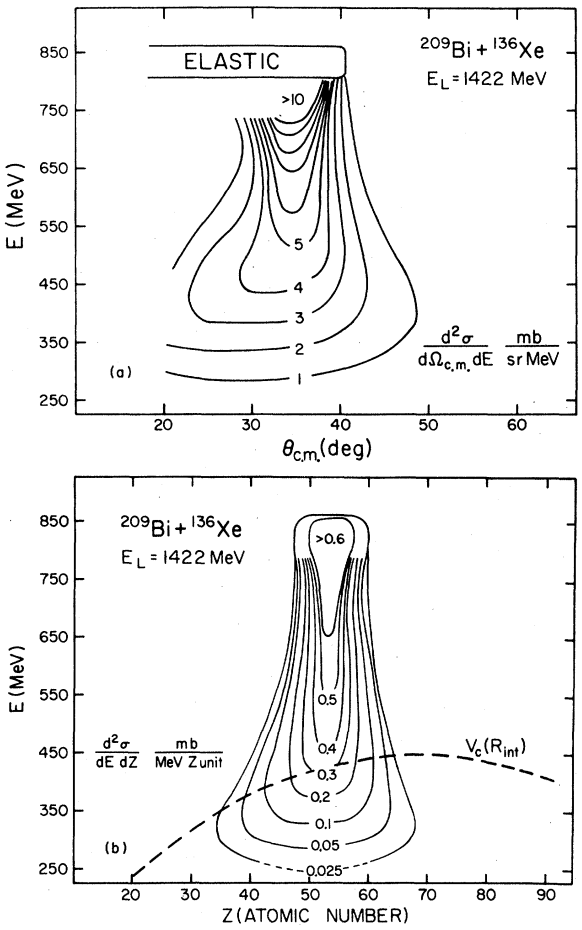

FIG. 6.. Gross features of the ^{209}Bi+^{136}Xe collision at a bombarding energy of 1422 MeV. (a) The double differential cross section $d^2\sigma/d\Omega_{c.m.}dE$ is plotted as a function of the center-of mass scattering angle and the total kinetic energy (Wilczyński diagram). (b) The double differential cross section $d^2\sigma/dE\,dZ$ is plotted as a function of nuclear charge (Z) and total kinetic energy (diffusion diagram). The Coulomb barrier of two touching spheres at the interaction radius $V_C(R_{int})$ is indicated by the dashed line.

section $d^2\sigma/dE\,d\Omega_{c.m.}$ and $d^2\sigma/dE\,dZ$, respectively. Both these diagrams are constructed from the same set of experimental data.

From the so-called Wilczyński diagram [Fig. 6(a)], which is obtained by plotting the double-differential cross section versus total kinetic energy E and center-of-mass scattering angle $\theta_{c.m.}$, one can study the evolution of the deflection function from the elastic ($E_{c.m.}=861$ MeV) to the fully relaxed component. In agreement with the previous measurements at lower bombarding energies the main feature of the E-$\theta_{c.m.}$ plot is the pronounced angular focusing of the reaction products. However, in the present experiment the distribution broadens markedly with increasing loss of kinetic energy and shows the development of a small contribution of an orbiting process. Several attempts[13–15] have been made to describe the gross feature of Wilczyński diagrams for a wide range of bombarding energies and systems in terms of a single parameter such as the modified Coulomb parameter η' or the modified angular velocity ξ. While not too much emphasis should be put on such attempts since the reaction is certainly too complex to be described by one parameter, it may be noted that the present experimental result is more consistent with the η' systematics[13] (Table I) than with the ξ-parameter representation,[15] which predicts a pronounced orbiting type reaction.

The diffusion diagram of Fig. 6(b) is derived from the same experimental data. However, the double-differential cross section is now presented as a function of the total kinetic energy E and the charge Z of the light fragment. At this high bombarding energy the element distribution can be investigated for Q values ranging from 0 to -575 MeV. The Z distribution develops from a narrow symmetric distribution and widens monotonically as the kinetic energy decreases. For a very large loss of kinetic energy, the centroid of the Z distribution is slightly shifted towards a more asymmetric fragmentation as compared to the entrance channel. Figure 6(b) also displays the Z dependence of the Coulomb energy $V_C(R_{int})$ (dashed curve) calculated for two spheres at a separation distance equal to the appropriate interaction radius. Measured kinetic energies much lower than V_C indicate large deformations of the intermediate system prior to breakup which become even larger for symmetric Z splits.

Following the above somewhat qualitative description of the data, Fig. 7 gives a quantitative representation of the element distribution. In this

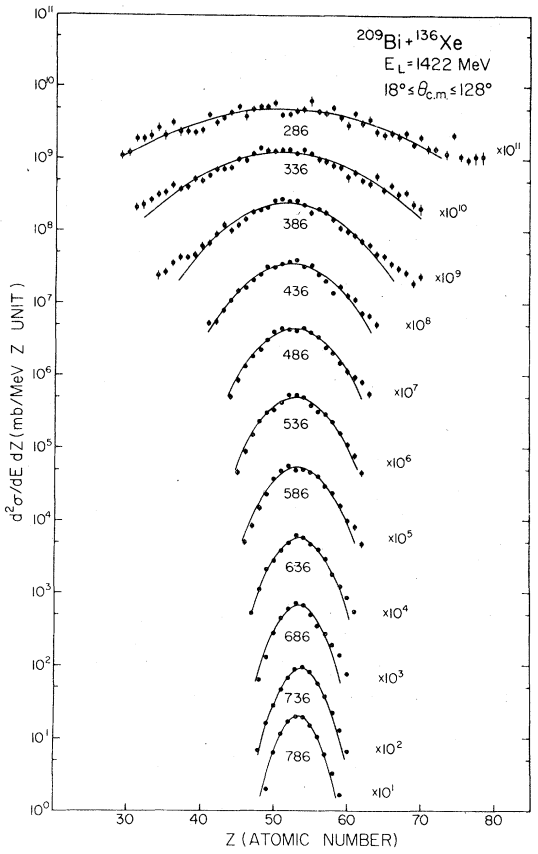

FIG. 7. Charge distributions are plotted for different values of the total kinetic energy as indicated in the figure. The width of each energy bin is 50 MeV. The solid curves are Gaussian least-squares fits to the data.

figure the double-differential cross section $d^2\sigma/dE\,dZ$, integrated over center-of-mass scattering angles from 18° to 128°, is plotted versus Z as a function of the final total kinetic energy E. Remarkably, the Z distributions remain Gaussian at all energies as evidenced by the solid lines representing Gaussian fits to the data. The centroids $\langle Z\rangle$ and the variances $\sigma_Z{}^2$ of the Z distributions as determined from the fits are collected in Table II as functions of the total kinetic energy. The variances $\sigma_Z{}^2$ have been corrected for the finite Z resolution (4.4 units FWHM for $Z=54$) for elastic scattering.

The difficulty in comparing measured differential element distributions with predictions of a classical trajectory calculation is that it requires a quantity which is correlated with the unmeasurable impact parameter. For this purpose the negative Q value, or as it is also known, the total kinetic energy loss

TABLE II. For the ^{209}Bi+^{136}Xe reaction at E_{lab}=1422 MeV, the centroid angle $\langle\theta_{c.m.}\rangle$ of $d^2\sigma/d\Omega_{c.m.}dE$, the differential cross section $d\sigma/dE$, the centroid $\langle Z\rangle$, and variance σ_Z^2 of the fragment Z distribution are given for 12 bins of the total kinetic energy $E=E_{c.m.}+Q$ in the center-of-mass system. The variance σ_Z^2 is corrected for the experimental Z resolution. The cross section integrated over energy bins between 261 and 811 MeV accounts for 2.8 b.

E (MeV)	$-Q$ (MeV)	$\langle Z\rangle$	σ_Z^2	$d\sigma/dE$ (mb/MeV)	$\langle\theta_{c.m.}\rangle$ (deg)
786	75	53.4±0.1	1.7± 0.3	11.5	34.0
736	125	53.8±0.1	2.6± 0.3	5.7	34.2
686	175	53.4±0.1	$3.4^{1.5}_{0.9}$	4.6	34.4
636	225	53.5±0.1	5.7± 0.5	4.4	34.4
586	275	53.3±0.1	$8.9^{1.8}_{1.2}$	4.9	33.0
536	325	52.9±0.1	11.4± 1.1	5.1	32.8
486	375	52.7±0.1	$16.1^{1.7}_{1.4}$	5.3	32.4
436	425	52.2±0.1	25.2± 1.6	5.2	31.0
386	475	51.7±0.2	40.6± 2.7	4.4	28.8
336	525	51.1±0.3	82.4± 5.5	3.1	28.1
286	575	51.1±0.5	152 ±16	1.6	28.9

E_{loss}, has been used. Evidence has been presented earlier indicating that the total kinetic energy loss has a nearly linear dependence on the angular momentum,[1,2] at least on the average. The correlation between the measured variances of the Z distribution for various energy bins and the corresponding negative Q values is illustrated in Fig. 8 for the three bombarding energies. The error bars reflect the uncertainties in fitting Gaussian curves to the Z-distribution data. The variance increases smoothly with decreasing Q value and reaches the largest value when the kinetic energy is damped

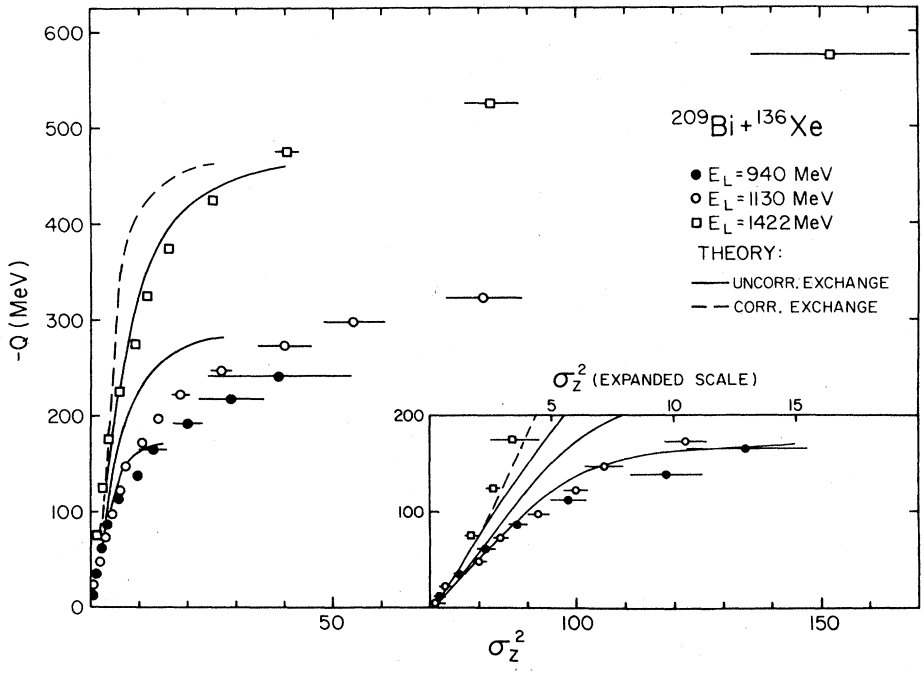

FIG. 8. The Q value vs σ_Z^2 correlations are shown for the ^{209}Bi+^{136}Xe system at E_{lab}=940, 1130, and 1422 MeV. The solid lines (uncorrelated nucleon exchange) and dashed line (correlated nucleon exchange) are results of dynamical calculations based on the proximity one-body transport model (Ref. 20).

down to fissionlike energies. For the present experiment the broadest element distributions of the $^{209}Bi+^{136}Xe$ reaction are observed, which is expected from the systematical behavior at the lower energies.

IV. COMPARISON WITH ONE-BODY TRANSPORT MODEL

A. Classical trajectory calculations

In Fig. 8 the experimental data for the $^{209}Bi+^{136}Xe$ reaction are compared to classical trajectory calculations, which have been very successful in the past both for the study of fusion[16,17] and strongly damped collisions.[3,17–19] In the present calculations use is made of a recently proposed nuclear potential[20] calculated from the surface energy of a dinuclear complex approximated by two spheres connected by a cylindrical neck and the proximity energy of surfaces outside the neck region. The nuclear one-body proximity friction form factor is modified[20] accordingly. The Coulomb potential is calculated with a phenomenological formula suggested by Bondorf *et al.*[21] The model ascribes energy dissipation and mass transport to the exchange of individual nucleons between two interacting nuclei approximated by two Fermi-Dirac gases. The current of exchanged nucleons depends on the occupancy of the single-particle orbits. Thus the Pauli blocking effect[3] has to be taken into account especially for reactions close to the Coulomb barrier. Further details of the calculations are described elsewhere.[3,15,19,20]

The one-body mechanism gives rise to finite widths of mass and charge distributions, due to the statistical nature of nucleon exchange. Regarding the nucleon exchange process as a random-walk process, the total number N of exchanged nucleons is related to the variance σ_A^2 of the mass distribution according to $\sigma_A^2=N$. Since in the present experiments only the variance σ_A^2 of the Z distribution is measured, the ratio σ_A^2/σ_Z^2 must be inferred. If the probability for a given transfer is independent of whether the nucleon is a proton or a neutron, $\sigma_A^2=(A/Z)\sigma_Z^2$, where the factor A/Z reflects the relative abundance of protons and neutrons. Experiments in which mass and charge are measured simultaneously, however, show that uncorrelated nucleon exchange does not occur and that the underlying potential energy surface has to be taken into account.[22–25] This leads to a more complex relation between σ_A^2 and σ_Z^2. Calculations for both correlated and uncorrelated particle exchange are shown in Fig. 8 for the present experiment at $E_{lab}=1422$ MeV. The data for the three bombarding energies are well represented by the theory for Q values down to the initially available kinetic energy, i.e., $-Q=E_{c.m.}-V_C(R_{int})$. However, systematic discrepancies remain between theory and experiment for large negative Q values which are not surprising in view of the various simplifications of the model.

In Fig. 9 the centroids of the c.m. angular distributions for different energy bins are plotted against negative Q values for the three experiments at $E_{lab}=940$, 1130, and 1422 MeV. Since the Q value is presumably related to the initial angular momentum,[1,2,15] these diagrams are closely related to the experimental deflection functions. As can be seen from Fig. 9, the one-body transport model (full curve) gives a reasonable reproduction of the experimental data, except for large negative Q values. It should, however, be pointed out that for an incident energy of $E_{lab}=1422$ MeV the model is unable to describe the dependence of the Q value

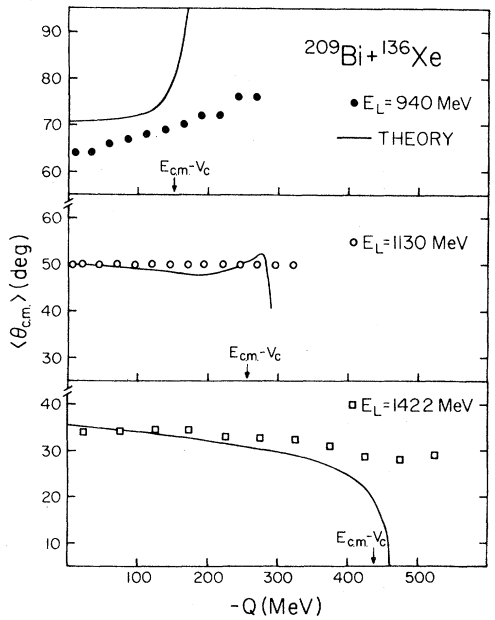

FIG. 9. Centroids of the angular distributions are plotted as a function of the Q value for the $^{209}Bi+^{136}Xe$ reaction at $E_{lab}=940$, 1130, and 1422 MeV. The experimental data are compared with predicted values (solid curve) of classical trajectory calculations at each energy (see text).

and the c.m. scattering angle on initial angular momentum if the latter is derived with the procedure outlined in Refs. 1 and 15. Possible reasons for this discrepancy could be that the conservative potential is in reality more repulsive for $E_{lab}=1422$ MeV than for the two lower bombarding energies or that energy dissipation associated with the neck motion is overestimated in the calculation. The agreement between theory and experiment in Fig. 9, which shows only the correlation between directly measurable quantities, is achieved because both discrepancies cancel in this diagram. Hence, if the method[1,15] of angular momentum decomposition is accepted, one is led to the conclusion that the three experiments cannot be reproduced with the unique set of conservative and dissipative forces assumed by the model. Further investigations are required in order to determine whether (i) the way the angular momentum is extracted from the data or (ii) unjustified model assumptions are responsible for the significant deviation between the predicted and derived correlations of the experimental observables with initial angular momentum.

B. Correlation between energy dissipation and nucleon exchange

A characteristic feature of the dynamical calculations, the Pauli blocking effect, that has been found[2] to play a crucial role in the ^{209}Bi+^{136}Xe reaction at 940 MeV, will be discussed in some detail in the following. This quantal effect is expected to be less important at $E_{lab}=1422$ MeV than at lower incident energies. Hence, the availability of data for one system at three different bombarding energies allows a crucial test on the presence of this effect. In a phenomenological approximation based on the one-body transport model,[1] the dissipated energy E_{loss} is correlated with the variance $\sigma_Z{}^2$ of the element distribution. It is given by

$$E_{loss}\equiv -Q = (E_{c.m.}-V_C)\times\left\{1-\exp\left[-\alpha\frac{m}{\mu}\left[\frac{A}{Z}\right]^x\sigma_Z{}^2\right]\right\}, \quad (3)$$

where $E_{c.m.}$ is the incident energy, V_C is the Coulomb energy of two spherical nuclei in the entrance channel, m and μ are the nucleon mass and the reduced mass of the system, respectively, and $x=1$ and $x=2$ represent assumptions of uncorrelated and correlated proton and neutron exchange, respectively. The quantity A/Z corresponds to the average fragment mass-to-charge ratio minimizing the potential energy, in the present case well approximated by that of the combined system. The coefficient α contains information on the character of the dissipation mechanism. It has been observed in the previous measurements at $E_{lab}=940$ and 1130 MeV that α decreases from 3.0 to 1.4 (if $x=2$) as the bombarding energy is increased. In a recently discussed quantal transport model[3] the Fermi-Dirac nature of the nucleons is taken explicitly into account. The Pauli principle restricts the exchange of nucleons between the colliding nuclei to transfer from occupied to unoccupied single-particle orbits. Therefore, at slow relative motion of the nuclei the exchange of nucleons is limited to the surface region of the Fermi spheres, since the volume of momentum space simultaneously occupied by both nuclei cannot contribute to the nucleon exchange. The flux of nucleons through the window that opens up in the neck between the two nuclei is reduced by a factor $1/\alpha<1$ as compared to the value derived on the basis of a classical-gas picture. For higher bombarding energies, the relative velocity of the two collision partners displaces the Fermi momentum spheres of the two nuclei and hence reduces the overlap region in momentum space. Therefore, the α parameter measuring this overlap region should be larger for bombarding energies close to the Coulomb barrier and decreases towards the classical limit $\alpha=1$ as the bombarding energy is increased, a trend observed in previous measurements. Figure 10 shows an experimental plot of $\ln T_0/T$ versus $\sigma_Z{}^2$ for the ^{209}Bi+^{136}Xe reaction at $E_{lab}=940$, 1130, and 1422 MeV, where $T_0=E_{c.m.}-V_C$ and $T=E_{c.m.}-V_C+Q$. As one can already see from this diagram, the results of the 940 MeV measurement clearly deviate from those at the two higher bombarding energies which nearly agree with each other within their experimental error bars. The observed linear relationship is expected from Eq. (3) with a slope given by $(m/\mu)(A/Z)^x\alpha$. The straight lines are least-squares fits to the data and the experimental slopes are listed in Table III. They are compared to predicted ones, where the α parameter is calculated as suggested by Wilcke.[2] As was demonstrated from the earlier experiments the bombarding-energy dependence of the slope can be reasonably well reproduced with the assumption of correlated nucleon exchange ($x=2$) and the introduction of Pauli blocking.

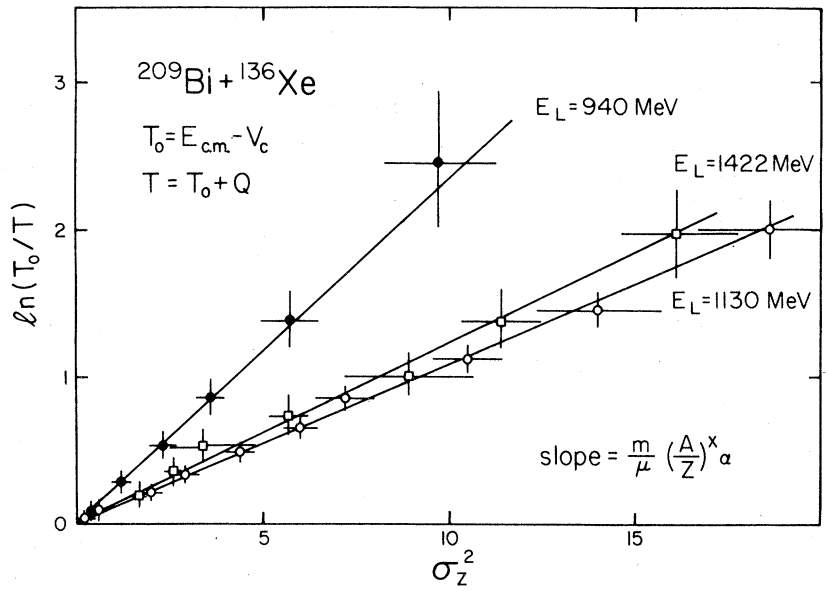

FIG. 10. The quantity $\ln(T_0/T)$ is plotted as a function of the variance σ_Z^2 for the $^{209}Bi + ^{136}Xe$ reaction at three bombarding energies. The quantity T_0 is the initial available energy above the Coulomb barrier, while T is the available energy for each Q value. The straight lines are least-squares fits to the data.

V. CONCLUSIONS

The $^{209}Bi + ^{136}Xe$ reaction studied in this work at a bombarding energy of 1422 MeV has provided, in connection with two previous experiments at 940 and 1130 MeV, detailed information on the bombarding-energy dependence of the damped reaction mechanism. The angular distribution of the Xe-like fragments is sideways peaked with its maximum near the quarter-point angle. Such an angular distribution consisting of a wide range of Q values indicates a delicate balance between repulsive and attractive forces as was found in previous experiments. The distributions measured in the three experiments can be characterized by Wilczyński plots which change remarkably little over a bombarding energy range from 1.9 to 5.3 MeV/nucleon above the Coulomb barrier in the entrance channel.

The maximum amount of energy damped in these heavy ion collisions is found to be approximately equal to the difference between the initial kinetic energy and the Coulomb barrier for a deformed system estimated from systematic studies of fissioning nuclei. For the investigated $^{209}Bi + ^{136}Xe$ reaction, independent of the bombarding energy, a

TABLE III. Comparison of experimental and theoretical slopes $(m/\mu)(A/Z)^x\alpha$ from the linear relation of $\ln(T_o/T)$ vs σ_Z^2 for the $^{209}Bi + ^{136}Xe$ reaction at $E_{lab} = 940$, 1130, and 1422 MeV. This slope measures the dissipated energy per nucleon exchange. the quantity μ/m is the reduced mass of the dinuclear system divided by the nucleon mass, $T_0 = E_{c.m.} - V_C(R_{int})$ and $T = E_{c.m.} - V_C(R_{int}) + Q$. For the extreme assumptions of uncorrelated and correlated proton and neutron exchange the values of x are 1 and 2, respectively. The quantal α parameter is calculated as suggested by Wilcke (Ref. 2).

E_{lab} (MeV)	Experimental slope (see Fig. 10)	Classical slope ($\alpha=1$)		Quantal slope	
		$x=1$	$x=2$	$x=1$	$x=2$
940	$0.23^{+0.06}_{-0.03}$	0.03	0.08	0.09	0.23
1130	0.11 ± 0.02	0.03	0.08	0.07	0.18
1422	$0.12^{+0.03}_{+0.02}$	0.03	0.08	0.05	0.14

minimum final total kinetic energy of ~270 MeV is observed. This energy is 150 MeV below the Coulomb barrier for spherical nuclei, indicating the occurrence of elongated dinuclear configurations in the exit channel.

The most striking observations made in the present experiment pertain to Gaussian-shaped element distributions which are studied down to a Q value of -575 MeV. Hence, these experimental data, as well as the results at lower bombarding energies, can be discussed in the framework of a simple diffusion model. Indications of a projectile splitting as inferred[11] from the asymmetric Z distributions of fragments from the $^{166}Er+^{86}Kr$ reaction at 12.1 MeV/nucleon are not seen in the present experiment.

Correlations between measured quantities such as final total kinetic energy, scattering angle, and charge of the projectilelike fragment are compared with theoretical predictions of a one-body transport model and are found to be in reasonable agreement with calculations, except for the largest Q values where the deformation of the intermediate system is underestimated. The Pauli blocking effect, observed to be significant for an understanding of the correlation between Q values and variances of the Z distributions for the 940 MeV data, is not quite as important at the highest bombarding energy, but its energy dependence is reflected in the three measurements.

ACKNOWLEDGMENTS

This work was supported by the U. S. Department of Energy. The authors would like to express their gratitude to the UNILAC staff for the efficient operation of the accelerator. Four of us (J.R.B., D.H., W.U.S., and W.W.W.) want to thank R. Bock and the Gesellschaft für Schwerionenforschung for the kind hospitality extended to them during their stay at Darmstadt. It is a pleasure for one of us (H.J.W.) to acknowledge helpful discussions with H. Emling. We thank A. D. Hoover for supplying us with unpublished $\Delta E/\Delta x$ data.

---

*Permanent address: Gesellschaft für Schwerionenforschung, D-6100 Darmstadt, Germany.
†Permanent address: Ruhr-Universität Bochum, D-4630, Germany.

[1]W. U. Schröder, J. R. Birkelund, J. R. Huizenga, K. L. Wolf, and V. E. Viola, Jr., Phys. Rep. 45C, 301 (1978).
[2]W. W. Wilcke, J. R. Birkelund, A. D. Hoover, J. R. Huizenga, W. U. Schröder, V. E. Viola, Jr., K. L. Wolf, and A. C. Mignerey, Phys. Rev. C 22, 128 (1980).
[3]W. U. Schröder, J. R. Birkelund, J. R. Huizenga, W. W. Wilcke, and J. Randrup, Phys. Rev. Lett. 44, 308 (1980).
[4]K. Braune, thesis, Max-Planck-Institut, Heidelberg, 1978 (unpublished); D. Schwalm (private communication).
[5]H. Essel, P. Sperr, K. Hartel, P. Kienle, H. J. Körner, K. E. Rehm, and W. Wagner, Nucl. Instrum. Methods 174, 515 (1980).
[6]D. Schwalm, A. Bamberger, P. G. Bizzeti, B. Povh, G. A. P. Engelbertink, J. W. Olness, and E. K. Warburton, Nucl. Phys. A192, 449 (1972).
[7]E. K. Warburton, J. W. Olness, and A. R. Poletti, Phys. Rev. 160, 938 (1967).
[8]J. B. Moulton, J. E. Stephenson, R. P. Schmitt, and G. J. Wozniak, Nucl. Instrum. Methods 157, 325 (1978).
[9]J. R. Birkelund, J. R. Huizenga, H. Freiesleben, K. L. Wolf, J. P. Unik, and V. E. Viola, Jr., Phys. Rev. C 13, 133 (1976).
[10]W. E. Frahn, Nucl. Phys. A302, 267 (1978).
[11]A. Olmi, U. Lynen, J. B. Natowitz, M. Dakowski, P. Doll, A. Gobbi, H. Sann, H. Stelzer, R. Bock, and D. Pelte, Phys. Rev. Lett. 44, 383 (1980).
[12]V. E. Viola, Jr., Nucl. Data Sect. A1, 391 (1966).
[13]J. Galin, J. Phys. (Paris) Colloq. C5, 37 (1976).
[14]G. J. Mathews, G. J. Wozniak, R. P. Schmitt, and L. G. Moretto, Z. Phys. A 283, 247 (1977).
[15]W. U. Schröder and J. R. Huizenga, Annu. Rev. Nucl. Sci. 27, 465 (1977).
[16]J. R. Birkelund, L. E. Tubbs, J. R. Huizenga, J. N. De, and D. Sperber, Phys. Rep. 56C, 107 (1979).
[17]D. H. E. Gross and H. Kalinowski, Phys. Rep. 45C, 175 (1978).
[18]H. H. Deubler and K. Dietrich, Phys. Lett. 56B, 241 (1975).
[19]W. U. Schröder, J. R. Huizenga, and J. Randrup, Phys. Lett. 98B, 355 (1981).
[20]E. S. Hernandez, W. D. Myers, J. Randrup, and B. Remaud, Lawrence Berkeley Laboratory Report LBL-9761, 1979.
[21]J. P. Bondorf, M. J. Sobel, and D. Sperber, Phys. Rep. 15C, 83 (1974).
[22]J. V. Kratz, W. Brückle, G. Franz, M. Schädel, I. Warnecke, G. Wirth, and M. Weis, Nucl. Phys. A332, 477 (1979).
[23]H. Breuer, B. G. Glagola, V. E. Viola, K. L. Wolf, A. C. Mignerey, J. R. Birkelund, D. Hilscher, A. D. Hoover, J. R. Huizenga, W. U. Schröder, and W. W. Wilcke, Phys. Rev. Lett. 43, 191 (1979).

[24]W. U. Schröder, J. R. Huizenga, and J. Randrup, Phys. Lett. 98B, 355 (1981).
[25]D. Schüll, W. C. Shen, H. Freiesleben, R. Bock, F. Busch, D. Bangert, W. Pfeffer, and F. Pühlhofer, Phys. Lett. 102B, 116 (1981).